35th Annual International Conference of the IEEE EMBS
Osaka, Japan, 3 - 7 July, 2013

REALISTIC BIOMECHANICAL MODEL OF A CANCEROUS BREAST FOR THE REGISTRATION OF PRONE TO SUPINE DEFORMATIONS*

Carolina Wessel, Julia A Schnabel and Sir Michael Brady

Abstract-- We develop a large deformations, Finite Elements biomechanical model of a stellate breast tumour, subject to prone to supine (MRI to US) breast deformations. Based on clinical findings, we introduce a volume of increased mammographic density/stiffness around a spiculated tumour, as well as a range of reported mechanical properties, both linear elastic and hyperelastic. This novel model demonstrates that these have a non-negligible effect on stresses and displacements, which, in turn, have implications, for example, in breast registration. We also show that the choice of material properties plays a dramatic effect on the mechanical variables.

I. INTRODUCTION

We develop a novel large deformations, Finite Element (FE) biomechanical model of a female cancerous breast for the registration of MR and US (prone to supine). A model of this type has multiple clinical applications, apart from registration, among which we can mention surgical planning and image-guided surgery.

Though modelling the overall structure of the breast is of interest, the structure of tumours and surrounding tissues is of utmost importance, yet, it has been neglected in previous models. With this in mind, this work incorporates two effects: the spiculated geometry of the vast majority of malignant breast tumours and the presence of mammographically dense/stiffer tissues in the vicinity of the tumour.

It has been reported [3] that over 90% of malignant breast tumours correspond to invasive carcinomas and show a characteristic "stellate" or "spiculated" geometry, observable in histopathological images and mammograms. The stellate nature of the vast majority of malignant tumours has a high positive predictive value of cancer [3], being a sign of invasive growth. Surprisingly, previous mechanical models of malignant tumours have ignored their spiculated geometry assuming, instead, a smooth tumoral surface. As we will show, this means that such models are not able to capture some of the essential biomechanics of tumours, not least for constraining deformable registration.

Ever since the pioneering work of John Wolfe, in 1976 [4], it has been accepted that there is a correlation between increased mammographic density and cancer risk. Mammographic density is characterized by a higher expression of collagen I and deregulated collagen metabolism, for example in the form of collagen cross-linking [5]. It has been shown that both increased collagen [6] and increased cross-linked collagen [7] promote tumorigenesis and invasion. These findings are of substantial relevance to this work, since, for example, Levental and co-workers in [7] showed experimentally that, in rats, increased collagen cross-linking is associated with incremental stiffening of mammary gland tissues during the transition from normal to premalignant to invasive cancer. They observed a three- to eight-fold increase in elastic modulus for unconfined compressions, for samples of premalignant tissues and tumours.

Another effect well known to clinicians is the pressure in the surface of tumours, that has dramatic clinical effects. Even if we have included surface pressures in previous models [1,2] lack of space hinders us from doing it here.

In the past we implemented a novel model of an isolated stellate breast tumour under mammographic compression forces [1, 2]. We show here that, also for a tumour embedded in a human breast, as well as for gravitational forces, the spiculated geometry of typical breast malignant tumours and the presence of stiffer tissues –both well known to clinicians but ignored to date in models- have a non-negligible effect on stresses and displacements. We also show the significant effect introduced by the choice of the material properties of the different breast tissues.

II. MATERIALS AND METHODS

Our large deformations, FE biomechanical model of a cancerous breast was implemented in Abaqus (www.simulia.com), as shown in Figure 1. Abaqus has enabled us to simulate large deformations and to vary material properties, mesh densities and tumour geometries without loss of precision. Abaqus has been used in the past in biomechanical applications [8, 9, 10].

The breast 3D geometry is reconstructed from an MR image using University of Utah software (http://www.sci.utah.edu): Seg3D for segmentation –of fatty and fibroglandular tissues- and SCIRun to create the geometry files. Given that during a MR scan the patient lies prone, MRI shows the breast deformed under gravity, which means that in a first step the gravitational force effects have to be subtracted, in order to generate the stress-free "reference" state. In a second step, since the patient lies supine while a US scan is performed, gravitational forces need to be applied again.

* C. Wessel and J. A. Schnabel are with the Institute of Biomedical Engineering, University of Oxford, OX3 7DQ, UK. Email:cwessel@robots.ox.ac.uk
Sir M. Brady is with the Department of Radiation Oncology and Biology, University of Oxford, OX3 7DQ, UK. Email: mike.brady@rob.ox.ac.uk

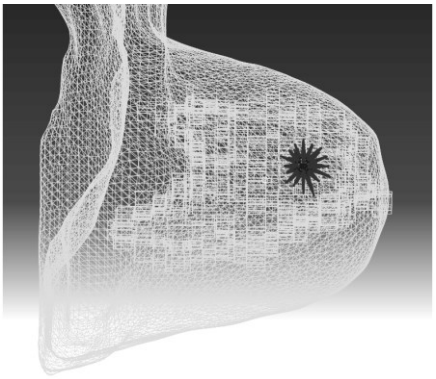

Figure 1. Meshed model that includes adipose and fibroglandular tissues as well as a stellate tumour (dark).

Our Abaqus model consists, thus, of two identical steps, in both of which gravity is applied in the same direction, keeping the breast fixed. In both steps, tissues were considered homogeneous, isotropic and incompressible. The density value used in this work is 1 g/cm^3, given the high water content of soft tissues.

We assume zero-tractions at breast-air interface nodes and zero-displacements at the breast-chest interface nodes, assuming that the patient does not move/breath during scans.

We have implemented three sets of material properties, -E2, PP and PA- both linear elastic and hyperelastic, as shown in Table 1. We have also explored other reported values [1] but found that they give rise to convergence issues or lead to physically unrealistic results.

Tetrahedral meshes were created in Abaqus for the mathematically created tumour [1,2] and for the adipose and fibroglandular tissues. After performing a convergence analysis (results not shown here), the final number of elements was, for the adipose tissue, 851890, for the fibroglandular tissue (in both breasts), 240617 and for the tumour, 198105.

Noted above, we have analysed the effect of spiculated (as opposed to smooth) tumours, as well as the effect of mammographically dense/stiffer tissues. Table 2 summarises this, so that, Case A corresponds to a smooth tumour, Case B corresponds to a stellate tumour, while Case CN corresponds to a spiculated tumour surrounded by a fully stiffer fibroglandular tissue volume, that is, where the material properties correspond to the average between normal fibroglandular and tumour. We note here that the choice of a fully stiffer fibroglandular tissue volume is probably not realistic. However, since malignant tumours are usually located in areas of high density/stiffness, and these areas may, in some cases, be significantly large, CN would correspond to the most extreme case.

In each case, the relevant mechanical variables are von Mises stresses σ_{vm} [Pa] and displacement modulus u [mm], where σ_{vm} was chosen, not as a measure of fracture (as traditionally), but as a scalar that captures the complexity of the stress tensor. These variables were calculated at two paths (Figure 2, (a) and (b)): path-esp and path-nipple.

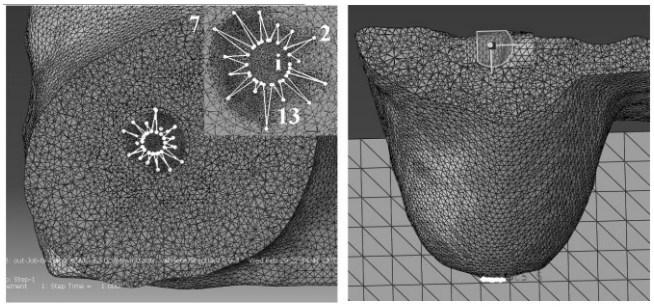

Figure 2. (a) path-esp includes nodes in the core and in the tips of the spicules in the tumour, such as nodes i, 2, 7 and 13. Path-esp is perpendicular to the gravitational force (b) path-nipple includes nodes at the nipple. Both paths are located in the right breast.

Path-esp, perpendicular to the gravitational force, includes nodes in the core and in the tips of the spicules in the tumour or the corresponding nodes for smooth tumours. Path-nipple only includes nodes in the right nipple, located, obviously in the right breast, where we have placed the tumour. We should note here that we have varied the position of the tumour, even if lack of space hinders us from showing the results here.

III. RESULTS

The following tables show the values of σ_{vm} [Pa], displacement modulus u [mm] as well as the corresponding percentage relative differences Δ.

1. Comparison of smooth and stellate tumours.

Table 3 shows the von Mises stresses σ_{vm} for smooth (A) and stellate (B) masses in path-esp, nodes 2, 7 and 13 (Figure 2). Table 3 (a) corresponds to the linear elastic set of material properties (E2), (b) to the first hyperelastic set (PP) and (c) to the second hyperelastic set (PA). Table 3 clearly demonstrates the dramatic increase in stresses generated by spiculated tumours. As shown for the isolated tumour in [1,2], the increase in stresses is more evident for the latter set of materials, emphasising the importance of the chosen material properties for the breast tissues. We should note here that this dramatic effect can be observed even for relatively small forces, such as the gravitational load.

Table 1. Different sets of material properties analysed and compared in this work.

Name	Type of fit	Glandular and fatty tissues	Malignant tumours
E2	Linear elastic	Linear elastic [11]	Linear elastic [11]
PA	Hyper elastic	Polynomial-quadratic [12]	Arruda-Boyce [13]

PP	Hyperelastic	Polynomial-quadratic [12]	Polynomial-quadratic [13]

Table 2. Cases analysed and compared.

CASES	Description
A	Smooth tumour
B	Stellate tumour
CN	Stellate tumour surrounded by stiffer fibroglandular tissue

The presence of the spicules generates small differences in displacements of the tumour -below 5%-, so that they are not shown here. That the stellate geometry of the tumours does not seem to introduce a significant difference in displacements is not fully surprising, since the spicules in case B only introduce a small volume increase to the tumour, yielding a small difference in displacements. A similar argument could be made about the small relative percent difference between displacements at the nipple that are not significantly changed by the presence of spicules.

2. Comparison of stellate and stellate surrounded by stiffer tissue models (cases B and CN).

Table 4 shows the von Mises stresses for (a) the E2, (b) the PA and (c) the PP material properties, for the spiculated (B) and spiculated surrounded by stiffer tissue (CN), in path-esp, nodes 2, 7 and 13. In this table the values for B may be higher or lower than the values for CN, which shows that there is not a clear trend associated with the increase of stiffer tissue for the tumour embedded in a breast. Unlike those results shown in [1, 2] for the isolated tumour, the stress shield introduced by stiffer tissues may increase or decrease as the volume of stiffer tissues increase, suggesting that the geometry of the structure and the distance to the fibroglandular tissue and breast boundary may also play a role.

Comparison of Tables 4 (a), (b) and (c) show here again the significant increase in stresses for the PA and PP sets of materials, highlighting here again the importance of the choice of material properties.

Table 5 shows the values of the modulus of the displacements u [mm] for the node i (see Figure 2) at the core, that will inform us of the general displacements of the tumour.

Table 3. von Mises stresses σ_{vm} for smooth (A) and stellate (B) masses, (a) for E2. (b) for PP and (c) for PA, respectively.

(a)	path-esp	σ_{vm}	
E2	A	B	ΔAB
NODE 2	1838	27977	1422
NODE 7	1119	11299	910
NODE 13	1476	21653	1367
(b)	path-esp	σ_{vm}	
PP	A	B	ΔAB
NODE 2	1370	615983	44853
NODE 7	1431	287623	19993
NODE 13	1397	93176	6568
(c)	path-esp	σ_{vm}	
PA	A	B	ΔAB
NODE 2	1370	642125	46760
NODE 7	1431	296358	20603
NODE 13	1397	89504	6305

Table 5 clearly shows the decrease in displacements due to the presence of a stiffer fibroglandular volume, confirming here the need to include stiffer tissues in a realistic breast model. The extent of the mammographically dense or stiffer tissue should be determined for each individual patient, as well.

Table 5 also shows that the results vary for the E2 and PP and PA sets of materials, making here again the choice of material properties significant.

Finally, Table 6 shows the modulus of the displacements at the right nipple, averaged for all the nodes. It may be observed that there is a significant decrease in displacements for the CN case. Not only are displacements smaller for but also the values of ΔBCN are higher for the E2 set of material properties, highlighting here again the importance of the chosen material properties, if a purely mechanical registration of the prone to supine deformations were made, and the need to include these effects in a realistic model.

Table 4 von Mises stresses σ_{vm} for and stellate (B) masses and and stellate surrounded by stiffer tissue (CN), (a) for E2. (b) for PP and (c) for PA, respectively.

(a)	path-esp	σ_{vm}	
E2	B	CN	ΔBCN
NODE 2	27977	15249	-45
NODE 7	11299	10665	-6
NODE 13	21653	8478	-61
(b)	path-esp	σ_{vm}	
PP	B	CN	ΔBCN
NODE 2	615983	449018	-27
NODE 7	287621	469934	63
NODE 13	93176	274095	194
(c)	path-esp	σ_{vm}	
PA	B	CN	ΔBCN
NODE 2	642125	570705	-11
NODE 7	287623	469944	63
NODE 13	89504	338184	278

Table 5. Modulus of the displacements u [mm] for a stellate (B) mass and and stellate surrounded by stiffer tissue (CN), (a) for E2. (b) for PP and (c) for PA, respectively.

(a)	path-esp	u	
E2	B	CN	ΔBCN
NODE i	3.0	2.5	-16.6

(b)	path-esp	*u*	
PP	B	CN	ΔBCN
NODE i	7.9	4.6	-42.4
(c)	path-esp	*u*	
PA	B	CN	ΔBCN
NODE i	7.9	4.6	-42.4

Table 6. Modulus of the displacements *u* [mm] for a stellate (B) mass and and stellate surrounded by stiffer tissue (CN), (a) for E2. (b) for PP and (c) for PA, respectively.

(a)	path-nipple	*u*	
E2	B	CN	ΔBCN
	5.5	4.6	-15.3
(b)	path-nipple	*u*	
PP	B	CN	ΔBCN
	14.0	9.3	-33.5
(c)	path-nipple	*u*	
PA	B	CN	ΔBCN
	14.0	9.3	-33.5

IV. CONCLUSIONS

Comparison of smooth and stellate tumours shows that the von Mises stresses increase dramatically for the spiculated tumours. Moreover, this increase can be observed for relatively small forces, such as the gravitational load. However, the displacements at the right nipple as well as the tumour do not vary significantly, whether the tumour is smooth or spiculated.

The increase of stiffer tissue volume around the tumour results in a decrease of the displacements of the tumour, as well as a difference in stresses. However, this decrease does not necessarily increase for "stiffer" tissue volume.

Comparison between stellate and stellate plus stiffer tissue tumours shows that the increase of stiffer tissue volume around the tumour results in a decrease of the displacements of the right breast nipple, where the tumour is embedded. We conclude that to realistically model the breast biomechanical response, the material properties and the extent of the mammographically dense or stiffer tissue should be determined for each individual patient.

Extremely important for this work, for all the analysed cases, both the displacements and stresses vary significantly for the three sets of material properties. This leads us to conclude that the registration of prone to supine for a random patient would, then, render completely different results for any of the three different material sets -taken from the literature- and none of these may even give the correct results. This highlights the need for patient-specific material properties and fits, if a purely mechanical registration is to be performed.

REFERENCES

[1] C. Wessel, J. A. Schnabel, M. Brady, "Towards a more realistic biomechanical modelling of breast malignant tumours." *Physics in Medicine and Biology,* vol. 57, pp 631-648, 2012.

[2] C. Wessel, J..A. Schnabel, and M. Brady,, "A Biomechanical model of spiculated tumours under mammographic compressions," *Engineering in Medicine and Biology Society (EMBC), 2010 Annual International Conference of the IEEE*, pp.712-715, Aug. 31 2010-Sept. 4 2010.

[3] P. Cherel, V. Becette, C. Hagay, "Stellate images: anatomic and radiologic correlations", *European Journal of Radiology*, Vol. 54, 37–54. 2005.

[4] J N Wolfe, "Breast patterns as an index of risk for developing breast cancer", *American Journal of Roentgenology*, Vol. 126, 1130-1137. 1976.

[5] D T Butcher, T Alliston and V M Weaver, "A tense situation: forcing tumour progression" *Nature Reviews Cancer*, Vol. 9 108-122. 2009.

[6] P P Provenzano, D R Inman, K W Eliceiri and P J Keely, "Matrix density-induced mechanoregulation of breast cell phenotype, signaling and gene expression through a FAK–ERK linkage." *Oncogene*. Vol. 10, no. 28, 4326–4343. 2009.

[7] K R Levental, H Yu, L Kass, J N Lakins, M Egeblad, J T Erler, S F T Fong, K Csiszar, A Giaccia, W Weninger, M Yamauchi, D L Gasser and V M Weaver, "Matrix crosslinking forces tumor progression by enhancing integrin signalling" *Cell*, Vol. 139, 891–906. 2009.

[8] A. O. Andrisano, E Dragoni and A Strozzi, "Axisymmetric Mechanical Analysis of Ceramic Heads for Total Hip Replacement", *Journal of Engineering in Medicine*, vol. 204, number 3 157-167. 1990.

[9] K. Ueno, J. W. Melvin, L.LI, and J. W. Lighthall. "Development of Tissue Level Brain Injury Criteria by Finite Element Analysis", *Journal of Neurotrauma*, Vol. 12, no. 4, 695-706. August 1995.

[10] A. Pérez del Palomar, B. Calvo, J. Herrero, J. López, M. Doblaré, "A Finite Element model to accurately predict real deformations of the breast", *Medical Engineering & Physics*, Vol. 30, Issue 9, 1089-1097. 2008.

[11] P. Wellman, R. D. Howe, E. Dalton, K. A. Kern, "Breast Tissue Stiffness in Compression is Correlated to Histological Diagnosis", Technical Report, Harward BioRobotics Laboratory, Harvard University, Cambridge, Mass, USA, 1999.

[12] A. Samani and D. Plewes. "A method to measure the hyperelastic parameters of ex vivo breast tissue samples". *Physics in Medicine and Biology*, Vol. 49, 4395-4405. 2004.

[13] J. J O'Hagan and A. Samani, "Measurement of the hyperelastic properties of 44 pathological ex vivo breast tissue samples", *Physics in Medicine and Biology*, Vol. 54, 2557. 2009.

Acknowledgements:

Sir Michael Brady and Carolina Wessel thank the CRUK/EPSRC for funding the Oxford Cancer Imaging Centre.